

Modeling of Uranyl Cation–Water Clusters

C. Clavaguéra-Sarrio,^{*,†} V. Brenner,[‡] S. Hoyau,[†] C. J. Marsden,[†] P. Millié,[‡] and J.-P. Dognon[‡]

LPQ, IRSAMC, Université Paul Sabatier, 118 route de Narbonne, 31 062 Toulouse Cedex 04, France, and DSM/DRECAM/SPAM-LFP (CEA-CNRS, URA 2453), CEA Saclay, 91 191 Gif-sur-Yvette Cedex, France

Received: November 4, 2002; In Final Form: January 22, 2003

Polarization and charge-transfer contributions have been shown to be nonnegligible in the binding energy of $[\text{UO}_2(\text{H}_2\text{O})]^{2+}$ and have been quantified by Coordination Energy Partitioning. In this context, two types of model potential for uranyl cation–water clusters, i.e., one including polarization effects explicitly and charge-transfer effects implicitly, and the other including these two effects explicitly, have been derived from ab initio calculations on $[\text{UO}_2(\text{H}_2\text{O})]^{2+}$. Only the model with the explicit charge-transfer term reproduces accurately the ab initio geometries and energies of small clusters containing up to five water molecules. An exploration of the potential energy surface of clusters with up to eight water molecules has been performed with the Monte Carlo growth method. The first coordination sphere in clusters contains five water molecules, as in experimental liquid and solid phases. The presence of further water molecules in the second and third coordination spheres reinforces the preference for five in the first shell. The coordination number five results from a subtle competition between polarization and repulsion contributions on one hand, which favor molecules in the second coordination sphere, and electrostatic and charge-transfer contributions on the other hand, which obviously favor molecules in the first coordination sphere. In addition, the water molecules in the second coordination sphere are principally oriented by a strong electrostatic interaction with the uranyl cation, but also interact weakly with two water molecules of the first coordination sphere.

1. Introduction

The safe management of highly radioactive spent fuel is currently a major challenge for the nuclear energy industry. Fundamental research is carried out in such areas as nuclear waste management and nuclear toxicology. These considerations imply that the solution chemistry of actinide compounds is of great interest. In the reprocessing strategy for nuclear waste, chemical processes are involved; at present, these are based on solvent extraction processes. In a first step, the PUREX process¹ is employed to separate the recyclable uranium and plutonium. After dissolution of nuclear fuel in aqueous nitric acid, uranium and plutonium are extracted in the form UO_2^{2+} and PuO_2^{2+} by TBP (tributyl phosphate). In this process, an extractant molecule (either as solvent or diluted in an organic solvent) is added to an aqueous solution containing ions to extract. This extractant molecule then forms complexes with uranyl and plutonyl cations, especially, which are confined to the organic phase, while the wastes containing all the other radioactive products remain in the aqueous solution. Such a complex chemical process clearly relies on a delicate balance between the different interactions which govern the system, particularly extractant molecule–cation and water–cation interactions. In this context, the water molecule not only acts as solvent, but it also plays a nonnegligible role in complex formation. One of the preliminary steps in understanding the solvent-extraction process consists of the study of the hydration of the uranyl cation, and more particularly of the structure of the first coordination sphere of this cation.

With a variety of spectroscopic and diffraction techniques (EXAFS,^{2,3} NMR,⁴ IR, and Raman⁵ or X-ray⁶), the most recent experimental data concerning the coordination properties of this cation in water indicate a coordination number of seven oxygens around the uranium in both liquid^{2–6} and solid phases:⁷ two oxygens of the uranyl cation and the five oxygens from water molecules. The only available experimental structural information in solution are the average bond distances, such as the uranium–oxygen distance ($\text{U}=\text{O}$) $1.78^2 - 1.76^3 - 1.70^6$ Å and the uranium–water distance ($\text{U}-\text{O}_w$) $2.41^{2,3} - 2.42^6$ Å (experimental uncertainties on the distances are about ± 0.01 Å), and two vibrational frequencies,⁵ the symmetric (870 cm^{-1}) and antisymmetric (961 cm^{-1}) stretching modes of the uranyl cation. In the past few years, the coordination properties of the uranyl cation in water have also been investigated in several theoretical studies.^{8–13} In the studies based on quantum chemical calculations,^{8–11} the relative stabilities of the $[\text{UO}_2(\text{H}_2\text{O})_{n=4-6}]^{2+}$ clusters were examined both in gas and liquid phases using various levels of theory for the calculation of the electronic energy (DFT^{8–10} or MP2/HF¹¹), and taking into account the bulk effects on both geometry and energies^{8,11} or only on energies^{9,10} with various solvent models. Qualitatively, all the liquid-phase results are in agreement and consistent with the experiments indicating a coordination number of five. However, there are a number of significant discrepancies between the results of these studies, illustrating the limits of such approaches: the difficulty both to explore the potential energy surface (PES) with ab initio calculations and to determine the number of water molecules which have to be explicitly included in the calculations. For example, Vallet et al.¹¹ have shown that explicit inclusion of second-shell water molecules, i.e., considering both structures such as $n + 0$ and $(n - m) + m$ (number of water molecules in

* Corresponding author. E-mail: carine.clavaguera@irsamc.ups-tlse.fr.

[†] LPQ, IRSAMC, Université Paul Sabatier.

[‡] DSM/DRECAM/SPAM-LFP (CEA-CNRS, URA 2453), CEA Saclay.

the first and second coordination spheres), is crucial for a proper analysis of the water exchange mechanism in such systems. Molecular modeling and simulation techniques such as Monte Carlo or molecular dynamics are then potentially more powerful for treating such problems, in particular to go beyond the first coordination shell water molecules. Moreover, such approaches facilitate the treatment of entropic effects, and molecular dynamics allows the study of time-dependent phenomena. The results obtained by these methods clearly depend on the quality of the model potential, which ideally should describe the several interactions in a balanced way. The first molecular dynamics simulations of the uranyl cation in water solvent have been performed by Guilbaud et al.¹² using a model potential based on the molecular mechanics AMBER force field, i.e., containing a Lennard-Jones term and a charge–charge interaction. However, Hemmingsen et al.¹³ have shown recently that such force fields cannot reproduce the *ab initio* curves of binding energies between the uranyl cation and two water molecules, suggesting that an appropriate force field must include polarization and charge-transfer effects.

We have decided to reexamine this general problem, and the challenge of this work is to elaborate an accurate model potential for uranyl cation–water clusters, investigating in particular the best way to introduce the polarization and charge-transfer contributions. We have, therefore, adapted the strategy based on *ab initio* calculations, developed and applied successfully to metal cation–water clusters (Na^+ , Cs^+ , Ca^{2+} , Ba^{2+} , La^{3+}) by Derepas et al.,¹⁴ to the specificity of the uranyl cation–water clusters.

The outline of this paper is as follows. We present first the strategy used to elaborate the model potential from *ab initio* calculations, especially in order to describe the uranyl cation–water interaction. In the following section, three parameter sets with an explicit treatment of the polarization contribution and either an implicit or an explicit treatment of the charge-transfer contribution are reported, and discussed in comparison with *ab initio* calculations on small clusters. Finally, using the best parameter set, we have performed a study of clusters of size up to 8 water molecules, to gain insight into the structure of the first coordination sphere, the role of supplementary water molecules on the uranyl cation–water interaction, as well as the nature of the main interactions between a water molecule lying in the second coordination sphere and its environment.

2. Methodology

2.1. Model Potential Strategy. We have used the model potential framework, as well as the strategy developed by Derepas et al.,¹⁴ to obtain model potential parameters from *ab initio* calculations. In such a model potential, the geometries of the molecules are kept frozen and all the dominant contributions (electrostatic, polarization, dispersion, dispersion-exchange, and repulsion-exchange) to the binding energy are expressed with simple analytical formulas, which are derived from a second-order exchange perturbation treatment. An important feature of this model potential is that the formulas used to describe the classic terms such as electrostatic and polarization ensure an accuracy at long distance equivalent to that obtained in reliable *ab initio* calculations. Moreover, the quantum terms such as dispersion and repulsion are described by sums of atom–atom terms, in which atom-dependent parameters are introduced. In this context, as the long-range behavior is by construction identical in the model potential and the *ab initio* calculations, only short-range interactions have to be fitted. The strategy consists then in extracting the atomic parameters of the quantum

terms from MP2 calculations performed on dimers: the water dimer for the oxygen and hydrogen atomic parameters and the metal cation with one water molecule for the metal cation parameters. In addition, as *ab initio* calculations take all the short-range effects into account which are not explicitly described in the model potential, such as charge-transfer or penetration, they are implicitly included as two-body terms. Obviously, the three-body terms due to dispersion and repulsion are neglected. As the model potential and the strategy have already been described in detail,¹⁴ we report here only the main characteristics and the changes we have carried out in order to describe the uranyl cation–water interaction.

In this framework, the uranyl cation is considered as a molecule and its geometry is frozen at the *ab initio* one. This assumption is quite reasonable since, as we shall see later (section 3.1), the U=O distance depends only weakly on its environment.

The electrostatic contribution is calculated as the sum of all two-body multipole–multipole interactions. A many-body treatment is implemented for the calculation of the polarization energy, including the back polarization contribution and the induced dipole-induced dipole interaction. The polarizable sites of each molecule correspond to the centers of the multipole distribution, and the associated isotropic dipolar polarizabilities were obtained from mean experimental values.¹⁵ For molecules with occupied d orbitals, such as the uranyl cation, the multipole multicentric development which gives the multipole distribution, used in ref 14, requires the multipole development to extend at least to the hexadecapole,^{16,17} and this implies a substantial increase of the computational cost in the calculation of the electrostatic–polarization interactions. We have therefore chosen to describe the electronic distribution of the uranyl cation and the water molecule by a multipole distribution containing a charge and a dipole on each atom, resulting from the fit of the *ab initio* electrostatic potential calculated at several van der Waals surfaces of the molecule.¹⁸ The polarizable sites are then the atoms, and because of the lack of gas-phase experimental data, the polarizabilities of the uranyl cation sites are obtained via a systematic scheme of redistribution of its *ab initio* molecular polarizability.¹⁵

The repulsion and dispersion terms are a sum of atom–atom interactions described by analytic expressions, derived from Kitaigorodskii's,¹⁹ with standard (i.e., non atom-dependent) parameters and two further atom-dependent parameters. In addition, the repulsion–dispersion terms take both the variation of the electronic population on each atom and its influence on the van der Waals radius into account, through a corrective factor G_{ij} expressed as $(1 - Q_i/n_i)(1 - Q_j/n_j)$. Usually, for light atoms such as oxygen or hydrogen, Q_i is taken as equal to the charge of the atom in the multipole distribution, and n_i as the number of valence electrons. It is this choice we have made for the oxygen and hydrogen atoms but not for uranium. In this last case, we have considered n_i as a supplementary parameter. Each atom is therefore defined by 2 or 3 parameters that need to be fitted.

The charge-transfer contribution is often nonnegligible, especially in the case of uranyl cation–molecule interactions. This short-range quantum term exhibits a priori both an n -body and a highly anisotropic character. However, only a few systematic representations of this term as an anisotropic n -body term have been proposed,^{20,21} and these models are in general not easily tractable when different orbital types by entity are involved in the electron-exchange process.²¹ In addition, when the charge-transfer term is not the dominant contribution to the

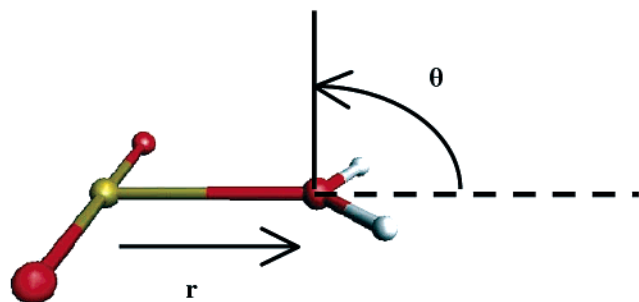


Figure 1. The two geometrical parameters considered for $[\text{UO}_2(\text{H}_2\text{O})]^{2+}$: the U–O_w distance r , which varies between 2.0 and 8.0 Å, and the dihedral angle θ (the angle between the UO_2^{2+} –O_w and the H_2O planes which varies between 0 and 90 degrees. The U atom is yellow.

binding energy, it can be considered as a two-body term.²² In this context, we have undertaken ab initio calculations (binding energy partitioning and population analysis) in order to check the order of magnitude of this term for the uranyl cation–water interaction, to identify the orbitals involved in the electron-exchange process, and to evaluate the charge-transfer anisotropy. In view of these results (see section 3.2), we have decided to check two strategies to take the charge-transfer between uranyl cation and water molecule into account: the first corresponds to an implicit treatment of this term (no supplementary parameters), while in the second it is introduced as a two-body uranyl cation–water isotropic term with two supplementary parameters.

We have chosen to use the atom-dependent parameters of the repulsion–dispersion terms found by Derepas et al.¹⁴ for the oxygen (uranyl cation or water) and hydrogen atoms. So the only unknown parameters are either the three parameters of the repulsion–dispersion terms for the uranium atom (pk , rz , n_u) in the case of an implicit charge-transfer term, or these three parameters plus two charge-transfer parameters (A , b) in case of an explicit charge-transfer term. The choice of the former atom-dependent parameters for oxygen and hydrogen atoms has been validated, by confirming that both the geometries and energetics of small water clusters are still correctly reproduced using them together with the new water multipole distribution. The parameters are then derived from comparisons with ab initio calculations performed at the MP2 level on a sample of configurations of the $[\text{UO}_2(\text{H}_2\text{O})]^{2+}$ cluster containing configurations both close to and relatively far from the equilibrium geometry of the first hydration shell. It is important to notice that the dispersion is often negligible in such charged clusters. The short-range interactions which are essentially fitted in this framework correspond to the repulsion and charge-transfer interactions.

2.2. Ab Initio Computational Details. *2.2.a. Interaction Energy Partitioning.* The Coordination Energy Partitioning (CEP) was performed for several configurations of the $[\text{UO}_2(\text{H}_2\text{O})]^{2+}$ cluster, varying the U–O_w distance and the angle θ between the UO_2^{2+} –O_w and H_2O planes (see Figure 1), this angle being important to evaluate the charge-transfer anisotropy. This method, based on the Reduced Variational Space (RVS) method first proposed by Fink²³ has been adapted by Clavaguéra et al.²⁴ to the MOLCAS package.²⁵ It enables the various contributions to the binding energy between two fragments to be determined at the Hartree–Fock level: the electrostatic, the repulsion, the polarization of each fragment, the charge-transfer from one fragment to the other, as well as the inverse charge-transfer contribution. Additional Natural Bond Orbital (NBO) population analyses have been performed with GAUSSIAN98²⁶

TABLE 1: Ab Initio, DFT, and Four-Components Results for the Free Uranyl Ion (The distance r_{eq} is given in Å and the vibrational harmonic frequencies ω_1 , ω_2 , and ω_3 are given in cm^{-1} .)

method	r_{eq}	ω_1	ω_3	ω_2
B3LYP no g^a	1.70	1025	1125	163
MP2 no g^a	1.75	922	1034	112
MP2 1 g^b	1.72	936	1047	144
4-CCSD (T) ^c	1.72	974	1121	164

^a Ref 28. ^b This work. ^c Ref 30.

at both the HF and MP2 levels in order to identify the orbitals involved in the electron exchange process. In all these calculations, the basis sets used are those described in the following section, i.e., those used in the MP2 calculations performed on small uranyl cation–water clusters.

2.2.b. Ab Initio Calculations on Small Clusters. To extract the parameter sets of the model potential, we have first performed single-point energy MP2 calculations on various configurations of $[\text{UO}_2(\text{H}_2\text{O})]^{2+}$, varying the U–O_w distance and the angle θ (see Figure 1). In these calculations, the geometries of the two fragments, the uranyl cation and the water molecule, are kept frozen, and the basis set superposition error (BSSE) was calculated for each configuration using the counterpoise (CP) approximation according to the method of Boys and Bernardi.²⁷ In this way, we obtained the potential energy surface corrected for BSSE. For the water molecule, large basis sets are derived from the van Duijneveldt primitive sets²⁸ and are equivalent to quadruple- ζ basis sets (O 14s7p/8s4p and H 10s/4s) augmented with two polarization functions (O 1.5, 0.35 and H 1.4, 0.25). It has been shown that these basis sets allow the experimental properties of the water molecule such as the geometry, dipole moment, ionization potential, and polarizability¹⁴ to be reproduced accurately at the MP2 level. For the uranyl cation, we have used the same basis set for the oxygen atoms and the basis set for the uranium atom is derived from the previous study of Ismail et al.²⁹ To describe scalar relativistic effects, the quasi-relativistic small-core pseudopotential of Stuttgart was used for U,³⁰ keeping 60 electrons in the core $[1s^2 2p^6 2s^2 2p^6 3s^2 3p^6 3d^{10} 4s^2 4p^6 4d^{10} 4f^{14}]$. The associated basis set was augmented by a g polarization function, the g exponent (0.85) being optimized on the uranyl cation MP2 energy, leading to the total basis set (10s11p9d8f1g/8s8p6d5f1g). The choice of adding a g polarization function was motivated by the results obtained by Ismail et al. which are reported with our results in Table 1. As already pointed out by Ismail et al., the MP2 calculations without a g polarization function on the uranium atom do not give accurate U=O distance and vibrational frequencies, in contrast with the B3LYP method. On the other hand, the addition of a g polarization function leads to the MP2 level results which reproduced well those obtained at a very high level of theory (a four-components CCSD(T) calculation).³¹ The MP2 calculations are also able to reproduce the second ionization potential of UO_2 , which is determined as 13.5 eV by the vertical energy difference between UO_2^+ and UO_2^{2+} ; this value is indistinguishable from the experimental result of 15.4 ± 2.6 eV.³² We have also used these basis sets at the MP2 level of theory to determine the data required for the calculation of the classical terms in the model potential (electrostatic and polarization contributions): the multipole distributions of the uranyl cation and the water molecule, as well as the polarizability of the uranyl cation. The multipole distributions are obtained with small RRMS errors on the MP2 electrostatic potential, about 0.05% for UO_2^{2+} and 3% for H_2O , respectively. Furthermore, the water dipole moment calculated

TABLE 2: MP2 Results for the $[\text{UO}_2(\text{H}_2\text{O})_{n=1-5}]^{2+}$ Clusters (The distances are in Å and the energies in kcal/mol. The relaxation error is the energetic percentage due to geometric relaxation. The first row gives the results for frozen geometries and the second row for full optimization.)

number of H_2O	symmetry point group	$d(\text{U}-\text{O}_w)$	$d(\text{U}=\text{O})$	binding energy (BE)	UO_2^{2+} BSSE	H_2O BSSE	total BSSE	corrected BE	relaxation error
1	C_{2v}	2.32	1.72	-67.5	0.6	1.0	1.6	-65.9	1.4
		2.31	1.74	-68.4	0.6	1.1	1.7	-66.7	
2	C_{2v}	2.35	1.72	-127.2	1.2	0.9	3.0	-124.2	1.0
		2.34	1.75	-128.9	1.2	1.1	3.4	-125.5	
3	D_{3h}	2.38	1.72	-180.0	1.7	1.1	5.0	-175.0	1.6
		2.37	1.76	-182.6	1.8	1.0	4.8	-177.8	
4	D_{4h}	2.41	1.72	-223.1	2.2	1.2	7.0	-216.1	1.5
		2.40	1.77	-226.5	2.3	1.2	7.1	-219.4	
5	D_5	2.47	1.72	-250.6	2.5	1.3	9.0	-241.6	1.5
		2.46	1.77	-254.3	2.6	1.3	9.1	-245.2	
4 + 1	C_1	2.41 ^a	1.72	-243.0	2.3	1.3 ^b	8.8	-234.2	2.6
		2.40 ^a	1.77	-249.4	2.4	1.3 ^b	8.9	-240.5	

^a Average of the different first coordination sphere U–O_w distances (2.39 Å, 2.41 Å, 2.42 Å, 2.42 Å in the frozen geometry and 2.39 Å, 2.39 Å, 2.41 Å, 2.41 Å in the full optimization). ^b Average of the H₂O BSSE (1.4 kcal/mol, 1.4 kcal/mol, 1.4, 1.4, and 0.9 kcal/mol in the frozen geometry and 0.7 kcal/mol, 0.7 kcal/mol, 1.9, 1.9, and 1.2 kcal/mol in the full optimization).

from the multipole distribution is very close to the ab initio result. Unlike the water molecule ($\alpha_L/\alpha_T = 0.80$), the polarizability tensor of the uranyl cation exhibits a high anisotropy: the longitudinal component α_L is 2.62 times larger than the transversal one α_T . However, the CEP calculations have shown that the uranyl polarization term is very small in comparison to that for water (see section 3.2). We can therefore expect that this approximation will be reasonable for the study of uranyl–water clusters.

MP2 calculations on both the $n + 0$ structures of small $[\text{UO}_2(\text{H}_2\text{O})_{n=1-5}]^{2+}$ clusters and the 4 + 1 structure of the cluster with five water molecules were carried out in order to determine their BSSE-corrected binding energies. In these calculations, the geometry of the fragments was first frozen to optimize intermolecular geometric parameters, and then all the coordinates were fully reoptimized, to obtain the relaxation effect on the binding energy. The BSSE was evaluated using the CP method. For example in the total optimization, for each molecule in the cluster, the BSSE is the energy difference between the energy of the molecule in the equilibrium geometry of the cluster obtained with the basis set of the molecule, and the energy of the molecule in the equilibrium geometry of the cluster obtained with the basis set of the whole system. We will see later that these calculations provide a severe selection criterion of the model potential parameter sets. Since MP2 calculations are hardly tractable for the cluster with six water molecules, only some relaxed calculations without any BSSE correction were performed with the DFT method (B3LYP functional) for this size.

All these calculations on small clusters have been performed with GAUSSIAN98.²⁶

2.3. Exploration of the Potential Energy Surface in Model Potential Calculations. To explore the PES, we have used the Monte Carlo growth method (MCGM)^{33,34} for $[\text{UO}_2(\text{H}_2\text{O})_n]^{2+}$ clusters ($n = 1$ to 8). A Boltzmann configuration set was generated at each size of the growth, using a fictitious temperature T . Starting from the configurations of a cluster of size n , the configurations of size $(n + 1)$ are obtained by the choice of 6 random coordinates, 3 for translation and 3 Euler angles for rotation, which allows the addition of the $(n + 1)$ th molecule. After this growth, all the configurations, selected at each size, are optimized by a local minimization algorithm³⁵ and the Hessian is calculated to confirm that the resulting stationary points are true minima. It is an efficient method to explore the main parts of the PES, first by varying the fictitious

temperature (T), and second by varying the details of the growth, i.e., the size when the uranyl cation is added. We have performed various growths for $T = 600$ K, 800 K, 1000 K, 1300 K, and 1500 K when the uranyl cation is the initial molecule, and for $T = 800$ K, 1000 K, and 1300 K for the uranyl cation added, for example, in the fourth position. Some tests have been performed when the uranyl cation is the last entity added to a water cluster, but no new stable structure has been found. All the structures obtained correspond to clusters in which the uranyl cation is surrounded by water molecules: a structure with the uranyl cation at the surface of the cluster was never observed.

3. Results and Discussion

3.1. Frozen and Relaxed ab Initio Calculations of Small Clusters. In Table 2, the ab initio MP2 results are given with the aim of showing the relaxation effects on geometries and interaction energies. The U–O_w variation with the relaxation is very small and corresponds to a systematic decrease of 0.01 Å, a value in the range of the uncertainties of experimental solution structure data. The U=O distance varies a little more, about 0.02–0.05 Å, and systematically increases with the number of H₂O molecules in the cluster. These variations are, however, not sufficient to influence the binding energies significantly, as can be seen from the relaxation binding energy percentage error which is always less than 3%; this observation justifies the use of a frozen geometry for the uranyl cation in the model potential. In addition, the trend from n to $n + 1$ in both the U–O_w distance and the energies of $n + 0$ structures is identical in frozen and relaxed ab initio calculations (see Table 3), as is the discontinuity obtained for the U–O_w distance between $n = 4$ and $n = 5$. In all these structures, we note that the angle θ is equal to zero. For $n = 2$, the symmetry point group is C_{2v} , corresponding to a competition between electrostatic and polarization contributions with an O_w–U–O_w angle of 107°. Less surprisingly, the symmetry point group is D_{3h} for $n = 3$ and D_{4h} for $n = 4$. For $n = 5$, the geometry is D_5 with a rotation of the water molecules around their own C_2 axis by 22°. The geometries and the binding energies in this series are very close to those found by Ismail with B3LYP calculations.³⁶ Extensive test calculations on other metallic cation complexes have already shown that the use of large basis sets is essential to reduce BSSE to typically 4% of the binding energy.³⁷ Thanks to the large and well-adapted basis sets used, the BSSE is reduced here to only 2% of the $[\text{UO}_2(\text{H}_2\text{O})]^{2+}$ binding energy. The MP2 binding energy difference between

TABLE 3: Changes in the U–O_w Distance (in angstroms) and in the Binding Energy Ratio, in Comparison to the Additive Model in Brackets, and Binding Energy Difference (size n minus size $n + 1$) on Increasing the Size of the [UO₂(H₂O) _{$n-1-5$}]²⁺ Clusters. Results of MP2 Optimization Calculations: First, with Frozen Intramolecular Geometries, and Second, with Fully Relaxed Geometries

method	cluster sizes	change in the U–O _w distance	change in the binding energy (additive model)	ΔE (kcal/mol)
MP2 frozen geometries	1–2	+0.03	1.89 (2)	58.4
	2–3	+0.04	1.42 (1.5)	50.7
	3–4	+0.03	1.24 (1.33)	41.3
	4–5	+0.06	1.12 (1.25)	25.4
MP2 relaxed geometries	1–2	+0.03	1.88	58.7
	2–3	+0.04	1.41	52.3
	3–4	+0.03	1.23	41.8
	4–5	+0.06	1.12	25.8

the lowest binding energy minimum 5 + 0 and the 4 + 1 structures is about 4.7 kcal/mol with full geometry optimization (and 7.4 kcal/mol for frozen geometry optimization), while the B3LYP binding energy difference between the lowest binding energy minimum 5 + 1 and the 6 + 0 complexes is about 10.7 kcal/mol (full geometry optimization); these results strongly suggest that five water molecules remain in the first coordination sphere, whatever the size of the cluster. In Table 3, we note that the binding energy ratio is always less than $(n + 1)/n$ in such clusters, in contrast to a simple additive model.

The relative energies of the 4 + 1 and 5 + 0 structures in the gas phase have already been considered by other groups, and the 6 + 0, 5 + 1, and 4 + 2 structures have also been compared.^{10,11} The results of these investigations do not always agree with our own, but it is important to note that different methodologies (methods and basis sets) were employed. Tsushima et al.¹⁰ report that the 4 + 1 species is slightly (0.4 kcal/mol) more stable than the 5 + 0, whereas the 5 + 1 is substantially (24.2 kcal/mol) more stable than the 6 + 0. The B3LYP method was employed in that work in conjunction with a 14 valence-electron pseudopotential; no symmetry constraints were imposed, and it is not clear to us from the figures whether the optimized structures in fact possess any symmetry higher than C_1 . Vallet et al.¹¹ report that the 5 + 0 species is more stable than the 4 + 1 by 7.0 kcal/mol, but they were not able to locate a 6 + 0 structure in the gas phase that is a true minimum. In that work, geometries were optimized at the SCF level and final energies obtained with the MP2 method.

We note that our comparison are broadly similar to those obtained by Vallet et al., but we are puzzled by the results reported by Tsushima et al. It is possible that the use of a 14 valence-electron pseudopotential, which is necessarily more restrictive than the 32 valence-electron pseudopotential we adopted, may be at least partly responsible. Concerning the possible existence of the 6 + 0 species, we note that we located it using a method that accounts for the larger part of the geometrical effects due to electron correlation, whereas Vallet et al. used only the SCF method for geometry optimization. We also remark that a 6 + 0 minimum was localized by Hay et al.,⁹ at the B3LYP level of theory. All authors agree that this species is unfavorable.

3.2. CEP Results. The NBO population analysis performed on the [UO₂(H₂O)]²⁺ cluster near its U–O_w equilibrium distance has shown that several different molecular orbitals are involved in the charge-transfer: for the uranyl cation, mainly 5f, 6d, and 7s orbitals of U, together with the lone pairs for the water molecule. The CEP method was first carried out starting from the equilibrium geometry of the [UO₂(H₂O)]²⁺ varying the

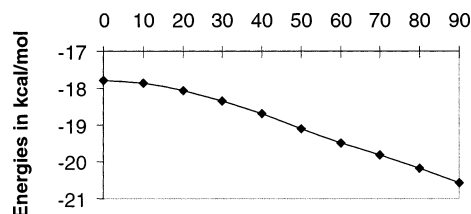


Figure 2. The energetic contribution due to charge-transfer in [UO₂(H₂O)]²⁺, as a function of the dihedral angle θ , for r (U–O_w) = 2.3 Å.

U–O_w distance. For U–O_w distances near the equilibrium value, even if the electrostatic contribution is the dominant term of the sum of the attractive contributions, both the polarization and charge-transfer effects are far from negligible. At 2.3 (2.5) Å, the polarization contribution has been evaluated to be 25% (24%) of the sum of the attractive contributions, and the charge-transfer 16% (13%). These observations justify our initial implicit treatment of the charge-transfer term (see section 2.1). In addition, these calculations have shown that both the polarization energy of the uranyl cation and the charge-transfer from it are much weaker than the corresponding water molecule terms: only 7% of the total polarization contribution and 2% of the total charge-transfer term at 2.3 Å. As expected, these CEP calculations confirmed that the charge-transfer contribution is a short-range term which decreases exponentially with the U–O_w distance. To check the anisotropy of the charge-transfer term, the CEP method was performed on configurations of [UO₂(H₂O)]²⁺ obtained by varying the angle θ (see Figure 1). Figure 2 shows the variation of the charge-transfer energy with the angle θ from the water molecule (the U–O_w distance is fixed at 2.3 Å). The charge-transfer energy varies slightly with the angle, but only by about 2 kcal/mol, corresponding to an anisotropy of about 10%. Strongly anisotropic contributions of the charge-transfer have been estimated by a more detailed partitioning, but due to their mutual compensation, the total charge-transfer is about isotropic.²⁴

We have thus introduced an isotropic two-body uranyl cation–water term, calculated as $-A \exp(-br)$ where r is the U–O_w distance, in the model potential with an explicit charge-transfer term. The b parameter is fitted to the charge-transfer contribution obtained with the CEP method ($b = 2.254 \text{ Å}^{-1}$). On the other hand, the A preexponential factor is fitted with the three other parameters of the uranium atom, i.e., on the MP2 calculations performed on [UO₂(H₂O)]²⁺, as SCF calculations often underestimate the charge-transfer term.

3.3. Choice of the Model Potential. We have used several selection criteria for the choice of the parameters sets of model potentials. The first one obviously consists of the agreement obtained for the geometry and the binding energy of the equilibrium structure of [UO₂(H₂O)]²⁺ as well as the agreement obtained for the binding energies between the model potential and the MP2 calculations on a sample of configurations of this cluster. Another results from the ability of the model potential parameters sets to reproduce the ab initio trends with the cluster size for both the U–O_w distance and energetics of the $n + 0$ structures up to $n = 5$. Finally, the last selection criterion is the coordination number of the uranyl cation, and in particular the ab initio binding energy separation between $n + 0$ and $(n - m) + m$ structures.

Initially, we tried to find a set of parameters containing only three parameters for the uranium atom, i.e., a model potential in which the charge-transfer was taken into account implicitly. Small RMS errors on the binding energies of the sample of configurations of [UO₂(H₂O)]²⁺ cluster as well as correct

TABLE 4: Results of Model Potential Calculations with the Three Sets of Parameters

set of parameters	cluster sizes	change in the U–O _w distance	change in the binding energy	ΔE (kcal/mol)
Set 1	1–2	+0.04	1.86	45.8
	2–3	+0.05	1.38	45.8
	3–4	+0.03	1.24	39.9
	4–5	+0.09 ^a	1.11	22.7
Set 2	1–2	+0.03	1.89	56.3
	2–3	+0.04	1.42	49.6
	3–4	+0.03	1.25	42.1
	4–5	+0.06	1.13	26.8
Set 3	1–2	+0.02	1.91	57.6
	2–3	+0.02	1.44	53.2
	3–4	+0.01	1.26	45.3
	4–5	+0.03	1.15	32.9

^a Average of the different U–O_w distances obtained (2.43 Å, 2.45 Å, 2.57 Å, 2.57 Å, 2.45 Å).

energetic and U–O_w distance of the equilibrium structure of this cluster have been obtained for the [UO₂(H₂O)]²⁺ cluster with several sets of parameters. However, all these sets give a nonzero angle θ for the [UO₂(H₂O)]²⁺ equilibrium structure with an average of 40°. The best set, corresponding to (*pk*, *rz*, *n_u* = 7.9, 1.2 Å, 14), called “set 1”, gives an equilibrium structure on the PES with an angle θ of 37°, a U–O_w distance of 2.32 Å, and a binding energy of –64.7 kcal/mol. The RMS error between the model potential and MP2 interaction energies obtained on the sample of configurations of [UO₂(H₂O)]²⁺ is only 4.4 kcal/mol. If we now consider the [UO₂(H₂O)_{*n*=2–5}]²⁺ clusters, the model potential reproduces correctly the O_w–U–O_w angles of the *n* + 0 structures, and in particular the angle of the cluster with two water molecules with a value of 100°. However, a nonzero angle θ is always found for these structures. In addition, in the 5 + 0 structure, the U–O_w distances are not equal for the five water molecules. Furthermore, if the model potential (Table 4) reproduces correctly the ab initio trend of the binding energy ratio with the increase of size (Table 3), it fails to predict the trend of the U–O_w distance satisfactorily. Finally, the coordination number obtained with the model potential differs from that of the ab initio calculation, since the model potential predicts that a 4 + 1 structure is more stable than the 5 + 0 structure by 4 kcal/mol.

Subsequently, in view of these results we decided to adopt an explicit treatment of the charge-transfer, which adds one parameter to the model potential. A set of parameters, called “set 2”, corresponding to (*pk*, *rz*, *n_u*, *A* = 4.7, 1.7 Å, 6, –4400 kcal/mol), gives an equilibrium structure with satisfactory values for both the binding energy (–63.2 kcal/mol) and the U–O_w distance (2.40 Å), but with an angle θ equal to 25°. The RMS error between the model potential and MP2 binding energies obtained for the sample configurations of [UO₂(H₂O)]²⁺ is small, and equal to 3.9 kcal/mol. This set corresponds to a strong (1 – *Q_i/n_i*) corrective factor for the uranium atom (*n_U* = 6). The trends for both the distance and the binding energy are now in very good agreement with MP2 results for the small clusters (Table 3 and Table 4); in particular the difference between the size four and five is correctly reproduced. Moreover, the O_w–U–O_w angles are always correctly reproduced, whatever the size of the cluster, and in particular, we obtained an angle of 108° for the [UO₂(H₂O)₂]²⁺ cluster. For this set, the coordination number of the uranyl cation is clearly five water molecules in the first coordination sphere: the 5 + 0 coordination is more stable than the 4 + 1 by 3.6 kcal/mol. All the selection criteria are respected, except for the persistent nonnegligible angle θ . Then we tried to obtain a set with an angle θ equal to zero.

This set, called “set 3”, corresponding to (*pk*, *rz*, *n_u*, *A* = 48.0, 1.0 Å, 92, –3800 kcal/mol) avoids the (1 – *Q_i/n_i*) correction for the uranium atom (*n_U* = 92). It gives a satisfactory binding energy (–63.3 kcal/mol) for the minimum, but the U–O_w distance (2.53 Å) is too long, and the RMS error between the model potential and MP2 binding energies obtained for the sample configurations of [UO₂(H₂O)]²⁺ is several times larger than before, at 10.3 kcal/mol. The O_w–U–O_w angles are well reproduced in the [UO₂(H₂O)_{*n*=1–5}]²⁺ clusters, in particular in [UO₂(H₂O)₂]²⁺ with a value of 103°. Nevertheless, the comparison of the trend of the U–O_w distance and the binding energy in the small clusters (Table 4) shows systematic discrepancies for the distance: the variations are too small. Another drawback for this set is the increase of the angle θ in clusters with two or more water molecules. Finally, even if the coordination number of the uranyl cation is clearly five water molecules in the first coordination sphere, the difference in energy of 10.4 kcal/mol between the 5 + 0 and the 4 + 1 coordination is slightly overestimated compared to the ab initio value.

It seems clear that the “set 2” is the most appropriate to model the uranium atom, despite a nonzero angle θ . If we now analyze in more detail both the model potential and the ab initio PES of the [UO₂(H₂O)]²⁺ cluster, we note that, along the angle θ , the model potential PES is too flat for short distances compared to the ab initio one. In the ab initio calculations, at 2.3 (or 2.5 Å), the structure with θ = 0° is 2.2 (or 1.4) kcal/mol more stable than the structure with θ = 30°. In the model potential calculations, the structure with θ = 30° is 0.4 kcal/mol more stable than if θ = 0° at 2.3 Å, whereas at 2.5 Å, the structure with θ = 0° becomes 0.2 kcal/mol more stable than if θ = 30°. This shortcoming cannot be due to the approximation used for the polarizability of the uranyl cation, since along this angle, the component involved in the calculation of the polarization corresponds to the same component, the α_T one. On the other hand, at 3 Å, the two PES along the angle become close and are finally identical at long distances, confirming that the model potential reproduces the long range terms, i.e., the electrostatic and the polarization energies, with a very good accuracy. We have therefore retained only this set of parameters to study in more detail the coordination number of the uranyl cation and the cation–water shell interactions in the last part of this work.

3.4. Analysis. *3.4.a. Number of Minima and Families of Structures.* For each size of cluster, it is possible to evaluate the number of minima between the lowest minimum and for example 98% of its binding energy. The results show that, for *n* = 1, 2, 3, and 4, the number of minima is only 1 or 2, but it increases to 9 for *n* = 5, to 16 for *n* = 6, to 34 for *n* = 7, and to 137 for *n* = 8. The number begins to increase quickly for *n* = 5 which is a first indication to define the coordination number.

The growths have revealed different families of structures (*n* + *m*) containing various isomers and corresponding to *n* molecules in the first coordination sphere and *m* molecules in other coordination spheres. The five-coordinated structures 5 + *m* are always the most stable (see Figure 3). The lowest 5 + 0 is more stable than the 4 + 1 family of structures by 3.6 kcal/mol. The lowest 5 + 1 is more stable than the 4 + 2 family of structures by 4.4 kcal/mol and is 8.5 kcal/mol below the 6 + 0 family of structures. The lowest 5 + 2 is more stable than the 4 + 3 family of structures by 5.6 kcal/mol, than the lowest 5 + 1 + 1 structure by 5.8 kcal/mol, and than the 6 + 1 family of structures by 11.2 kcal/mol. The lowest 5 + 3 is more stable than the 4 + 4 family of structures by 9.0 kcal/mol and than the 6 + 2 family of structures by 14.5 kcal/mol. So not only is

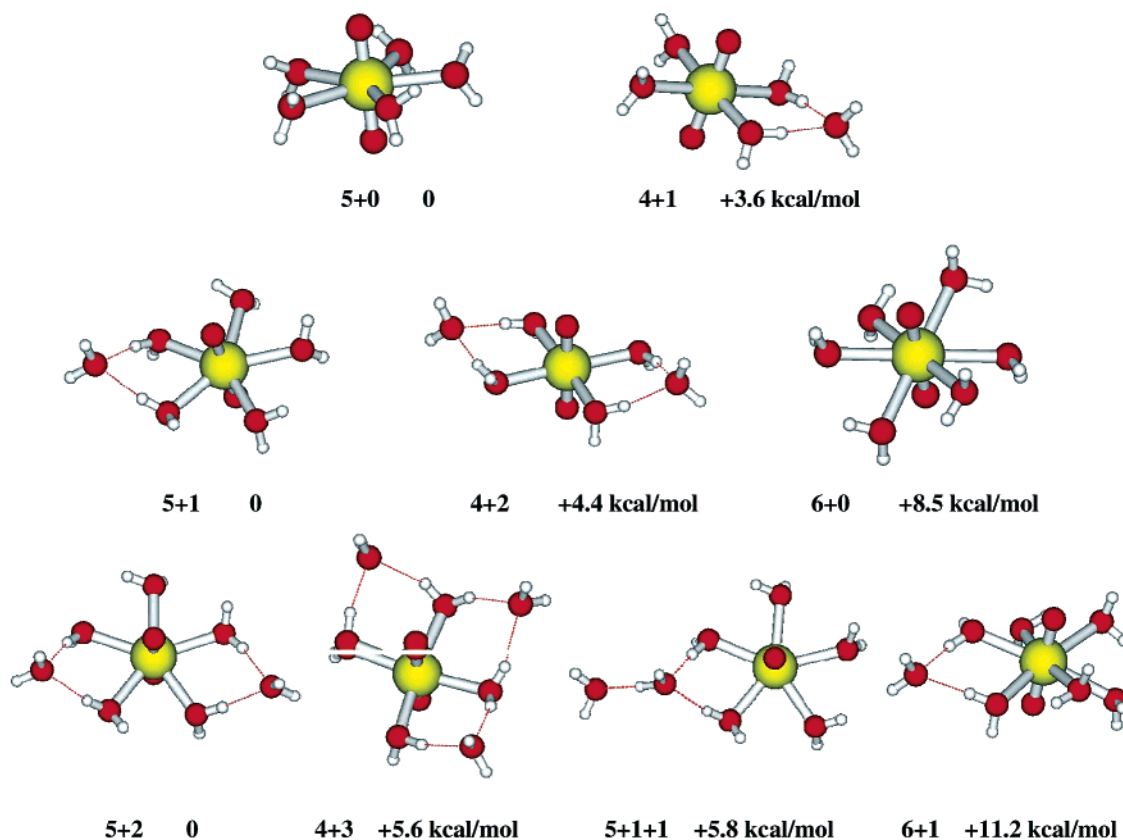


Figure 3. $[\text{UO}_2(\text{H}_2\text{O})_n]^{2+}$ conformations for $n = 5, 6$, and 7 . The model potential relative energies are given in kcal/mol compared to the binding energy of the absolute minimum for each size.

the coordination number five the most stable, but it is also further stabilized by adding water molecules in the second and third shells. One notes in Figure 3 that in the most stable structures, a water molecule in the second coordination sphere prefers to interact with two water molecules of the first coordination sphere, the oxygen atom of this molecule acting twice as a proton acceptor.

Looking at the $6+0$ structure given in Figure 3, we observe that the six water molecules are not in the equatorial plane of the uranyl cation, in contrast with the $5+0$ structure, that implies an increase of the $\text{U}-\text{O}_w$ distance (2.634 \AA for $6+0$ and 2.553 \AA for $5+0$). The $6+0$ geometry from the model potential was a successful starting point for B3LYP calculations and led to a minimum with three water molecules above the equatorial plane of the uranyl cation and three water molecules below it. The B3LYP structure is very close to the structure found by Hay et al.⁹ in which the uranyl cation is slightly bent, at 166° . In our model potential, the uranyl cation is frozen linear but the bending is not energetically expensive (only about 1 kcal/mol in our B3LYP calculations for a bend of 15°) due to the small value of the bending vibrational frequency ω_2 (Table 1).

3.4.b. Energetics. The coordination number of the uranyl cation can be confirmed by the detailed analysis of the various contributions to the binding energy. In Figure 4, the sum of the two-body contributions, polarization contribution and binding energy, are plotted for each global minimum in each size of cluster. For the size 6, each contribution of the structure $6+0$ is also reported with the symbol \star . It is clear that the slopes are changing for the two-body and the many-body contributions when going from the size 5 to 6. For n greater than 5, the supplementary water molecules go to the second coordination sphere and contribute less to the two-body terms: the first

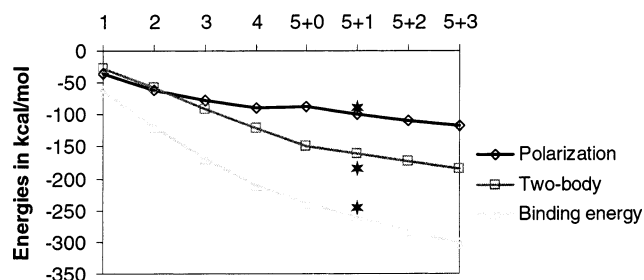


Figure 4. Trend of the binding energy, the sum of the two-body terms, and the polarization contribution on increasing the size of lowest minimum uranyl water clusters (\star for $6+0$ contributions, see the text for definition).

coordination sphere is complete. Moreover, the only many-body contribution, polarization, remains almost constant for one molecule before the first coordination sphere is completed, and then this contribution starts to increase again. Figure 5 shows the variation of the various two-body contributions: electrostatic, repulsion plus dispersion-exchange, dispersion, charge-transfer, and the sum of these terms. As expected, the dispersion contribution is quasi-negligible. The charge-transfer increases for $n = 1$ to 5 , but afterward, the slope is close to zero because the water molecules are kept away in the second coordination sphere and the charge-transfer contribution is negligible for these molecules. Moreover, the electrostatic component increases quasi-linearly. On the other hand, a change of slope at $n = 5$ can be seen for the repulsion contribution.

To understand the various interactions between the uranyl cation and the water molecules or between water molecules, we have compared the lowest cluster in each family, shown in Figure 3, for sizes 5 ($5+0$, $4+1$), 6 ($5+1$, $4+2$, $6+0$), and 7 ($5+2$, $4+3$, $5+1+1$, $6+1$). For each size, the

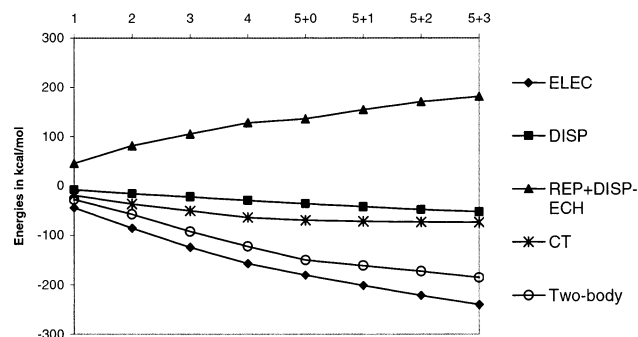


Figure 5. The two-body interactions: electrostatic, dispersion, repulsion plus dispersion–exchange, charge-transfer, and the sum of the two-body terms, as a function of the size of the uranyl–water cluster.

polarization contribution gives the same behavior: the more water molecules in the second or third coordination sphere, the larger the polarization term. For example, the polarization term is larger in the $4 + 2$ cluster than in the $5 + 1$, which is larger than in the $6 + 0$; the values are 112, 100, and 89 kcal/mol, respectively. On the other hand, the polarization contribution remains constant for the $4 + 0$, $5 + 0$, and $6 + 0$ structures (see Figure 4). The coordination number five results from a subtle competition between the principal components of the binding energy. Polarization and repulsion contributions favor structures with a water molecule in the second coordination sphere, such as $4 + 1$ and $5 + 1$ structures, while the electrostatic contribution and charge-transfer obviously favor structures with more water molecules in the first coordination sphere, such as $5 + 0$ and $6 + 0$ structures. If we compare the $4 + 1$ and $5 + 0$ structures, the difference in electrostatic terms dominates, whereas the polarization plus repulsion contribution is decisive for the $(5 + 1)/(6 + 0)$ comparison. These results lead to a coordination number five for the most stable minimum in each size of cluster. Moreover, in the $5 + 0$ structure, the five water molecules stay in the equatorial plane of the uranyl cation, despite both a nonnegligible Pauli repulsion of each water molecule with two neighboring water molecules (+1.6 kcal/mol for each pair so +8.0 kcal/mol for the whole cluster, in comparison with +0.2 kcal/mol for each pair so +0.8 kcal/mol for the $4 + 0$ cluster) and of repulsive electrostatic interactions of each water molecule with two neighboring water molecules (+1.0 kcal/mol for each pair so +5.0 kcal/mol for the whole cluster). These repulsions explain why no more than five water molecules can stay in the equatorial plane. In the $6 + 0$ structure, the six water molecules do not stay in this plane mainly because of the water–water repulsion contributions; these contributions are negligible for clusters up to 4 water molecules, but increase to 8.2 kcal/mol for the $5 + 0$ structure and to 21.4 kcal/mol for the $6 + 0$ structure.

In the following paragraph, the energies given are two-body interactions without the polarization contribution, to compare various water–water or water–cation interactions. A water molecule in the second coordination sphere has a relatively strong attractive interaction with the cation (for example, –16.3 kcal/mol in the $4 + 1$ cluster) compared to that of a water molecule in the first coordination sphere (for example, –28.5 kcal/mol in the $4 + 1$ cluster). Moreover, this interaction is essentially electrostatic, whereas the electrostatic and repulsion contributions are almost equal in magnitude in the first sphere (for example, –40.1 kcal/mol for electrostatic and +31.4 kcal/mol for repulsion in the $4 + 1$ cluster). In the $4 + 2$ structure, the interaction with the cation is about –16.4 kcal/mol but only –14.7 kcal/mol in the $5 + 1$ case, and it is stronger in the $4 + 2$ structure because of shorter U–O_w distances (in both the first

TABLE 5: Interaction Energies and Equilibrium M–O_w Distances for M^{q+}–(H₂O) Clusters (M^{q+} = Ca²⁺, UO₂²⁺, La³⁺) (Energies are in kcal/mol and the distances in Å.)

	Ca ²⁺ –(H ₂ O)	UO ₂ ²⁺ –(H ₂ O)	La ³⁺ –(H ₂ O)
<i>r</i> _{eq}	2.28	2.40	2.44
<i>E</i> _{int}	–54.6	–63.2	–82.2

and second coordination spheres). For the same reasons, the interaction between the uranyl cation and the water molecules in the second coordination sphere is larger in the $4 + m$ structure than in the $5 + (m - 1)$, which in turn is larger than in the $6 + (m - 2)$ case (for example, –17.1 kcal/mol for the $4 + 3$ cluster, –14.4 kcal/mol for the $5 + 2$ cluster, and –13.1 kcal/mol for the $6 + 1$ cluster). A water molecule in the third coordination sphere is attracted and oriented by the uranyl cation, this interaction still being larger than the water–water interaction (for example, in the $5 + 1 + 1$ structure, this interaction is –6.4 kcal/mol). The interaction of a water molecule in the second coordination sphere with a water molecule of the first coordination sphere is small (about –1.5 kcal/mol in the $4 + 1$ cluster) in comparison with the two-body interaction in the water dimer (–3.71 kcal/mol), and substantially weaker than the molecule–cation interaction.

One can notice that no cluster contains any water molecules that interact near the oxygen atoms of the uranyl cation with a hydrogen atom pointing to the oxygen atom of the uranyl cation such as in a hydrogen bond. We have performed some supplementary calculations in order to explore in detail the [UO₂(H₂O)]²⁺ PES corresponding to such configurations. For example, we have varied the O–H_w distance (from 1.0 to 7.0 Å) of a configuration in which one hydrogen atom (H_w) of the water molecule approaches one oxygen atom of the uranyl cation along its axis. Whatever the configuration, i.e., O–H_w distance and U–O–H_w angles, the binding energy is always repulsive, due to the fact that the water dipole is in the wrong orientation with respect to the uranyl cation. Hemmingsen et al. have obtained the same results from ab initio calculations on the [UO₂(H₂O)₂]²⁺ cluster.¹³ A simple electrostatic model which represents the uranyl cation by three point charges (+3 on U and –0.5 on each O, with 1.7 Å for the U=O distance) explains this observation. The potential, in appropriate units, can be expressed as $V \approx (2.5/(x + 1.7) - 0.5/x)$, and this is attractive only if x is less than 0.4 Å. Such a configuration is obviously impossible due to internuclear repulsive interaction, which is very strong at such short distances. These results confirm that such hydrogen bonds are inhibited at least for clusters up to eight water molecules, and consequently for any uranyl–water cluster.

3.4.c. Comparison with Two Other Cations: Ca²⁺ and La³⁺. It is interesting to compare the water–uranyl cation interactions with those between water and some simple metal cations such as Ca²⁺ and La³⁺.¹⁴ In Table 5, the interaction energies and the M–O_w equilibrium distances are given for the M^{q+}–(H₂O) clusters (M^{q+} = Ca²⁺, UO₂²⁺, La³⁺). In the model potential, the back polarization was taken into account for all three cations, but only the uranyl cation has an explicit charge-transfer. It is clear that the energetic and geometric parameters given for the uranyl cation complex are bracketed by those for Ca²⁺ and La³⁺. In Figure 6, the binding energy differences are plotted for the M^{q+}–(H₂O)_n clusters ($n = 8$ for UO₂²⁺ and $n = 9$ for Ca²⁺ and La³⁺). As for uranyl cation clusters, the binding energy ratio for Ca²⁺ and La³⁺ clusters is less than $(n + 1)/n$, in comparison to an additive model (see ref 14 and references therein). The energetic trend for the uranyl cation is close to that for Ca²⁺ when n is in the range 1–4, though the uranyl

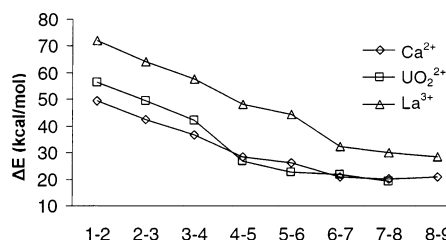


Figure 6. Variation of the binding energy differences on increasing the size of the $M^{q+}-(H_2O)_{n=1-8/9}$ clusters¹⁴ ($M^{q+} = Ca^{2+}, UO_2^{2+}, La^{3+}$).

cation values are somewhat larger, due to the charge-transfer contribution. But for sizes 5 and 6, addition of water molecules is less favorable for UO_2^{2+} than for Ca^{2+} , as a part of the coordination sphere is inaccessible. The coordination number of Ca^{2+} is six (octahedral geometry), corresponding to 4 water molecules in a plane, one water molecule above it, and one below it. For UO_2^{2+} , this structure is not possible due to the presence of the two “yl” oxygen. Afterward, the two curves are the same, because no further charge-transfer contributes to the binding energy in uranyl cation clusters. Despite the nonnegligible magnitude of the charge-transfer in the water uranyl cation clusters, the uranyl cation behaves rather like Ca^{2+} and the charge-transfer does not control the interaction. For La^{3+} clusters, the structure with 6 water molecules is octahedral, as for the Ca^{2+} , one, and it is energetically possible to add one water molecule in the first coordination sphere. The slope of the curve of the energy difference changes when the first coordination sphere is complete; it can be seen, for example, at size 6–7 in the lanthanum case. Intuitively, one can first anticipate a coordination number four of the uranyl cation in view of the results given for simple cations, but obviously, the uranyl cation coordination is more complex and its coordination number five, which has been studied in detail in this paper, is the only case characterized to date of a cation with 5 water molecules in the same plane.

Conclusions

We have presented here, for the first time to our knowledge, a model potential for uranyl cation water clusters which includes both polarization and charge-transfer effects. One of the most important points that must be emphasized here is that both polarization and charge-transfer have to be treated explicitly. The strategy used to elaborate this model potential from ab initio calculations on the $[UO_2(H_2O)]^{2+}$ cluster has been validated by the very good agreement obtained with ab initio energies and distances for small clusters. In agreement with other ab initio results and the first coordination sphere known in liquid and solid phases, we have found that the coordination of five water molecules in the first hydration sphere of the uranyl cation is the most stable in clusters up to 8 water molecules. An analysis of cation–water and water–water interactions has shown that water molecules are strongly oriented by the uranyl cation whether they are in the first, second, or third coordination sphere. In all the most stable structures, a water molecule in the second coordination sphere interacts with two water molecules in the first interaction sphere, and the magnitude of this interaction with each molecule is less than half of that in the water dimer. Moreover, the model potential proved to be useful to supply structures that were used to start quantum calculations. In this study, we have found a structure for the 6 + 0 cluster, not readily anticipated, which is a minimum in DFT calculations.

Despite these good results, a nonzero angle θ is found with our model. Further work is necessary to understand this

phenomenon more completely. As a first step, it seems necessary to describe the short-range behavior of the model potential more correctly by testing, for example, the quality of the repulsion term between the hydrogen atoms and UO_2^{2+} . It is also possible to explore the influence of repulsive polarization exchange and three-body terms.

In current work, we have introduced this model potential into a molecular dynamics program. Starting from Monte Carlo growth structures, we would like to consider temperature effects on the coordination number in small uranyl cation water clusters, and particularly on the 5 + 0, 4 + 1, and 6 + 0 structures. Moreover, we plan to study clusters up to 30 water molecules to learn more about the second coordination sphere, and it will be useful to plot $g(r)$ functions to estimate U–O_w and O_w–O_w distances to define this second coordination sphere.

References and Notes

- (1) McKibben, J. M. *Radiochim. Acta* **1984**, 36, 3.
- (2) Wahlgren, U.; Moll, H.; Grenthe, I.; Schimmelpfennig, B.; Maron, L.; Vallet, V.; Gropen, O. *J. Phys. Chem. A* **1999**, 103, 8257.
- (3) Allen, P. G.; Bucher, J. J.; Shuh, D. K.; Edelstein, N. M.; Reich, T. *Inorg. Chem.* **1997**, 36, 4676.
- (4) Bardin, N.; Rubini, P.; Madic, C. *Radiochim. Acta* **1998**, 83, 189.
- (5) Quilès, F.; Burneau, A. *Vib. Spectrosc.* **2000**, 23, 231.
- (6) Aberg, M.; Ferri, D.; Glaser, J.; Grenthe, I. *Inorg. Chem.* **1983**, 22, 3986.
- (7) Rogers, R. D.; Kurihara, L. K.; Benning, M. M. *J. Inclusion Phenom.* **1987**, 5, 645.
- (8) Spencer, S.; Gagliardi, L.; Handy, N. C.; Ioannou, A. G.; Skylaris, C. K.; Willets, A.; Simper, A. M. *J. Phys. Chem. A* **1999**, 103, 1831.
- (9) Hay, P. J.; Martin, R. L.; Schreckenbach, G. *J. Phys. Chem. A* **2000**, 104, 6259.
- (10) Tsushima, S.; Yang, T.; Suzuki, A. *Chem. Phys. Lett.* **2001**, 334, 365.
- (11) Vallet, V.; Wahlgren, U.; Schimmelpfennig, B.; Szabó, Z.; Grenthe, I. *J. Am. Chem. Soc.* **2001**, 123, 11999.
- (12) Guilbaud, P.; Wipff, G. *J. Phys. Chem.* **1993**, 97, 5645. (b) Guilbaud, P.; Wipff, G. *J. Mol. Struct.* **1996**, 366, 55.
- (13) Hemmingsen, L.; Amara, P.; Ansoborlo, E.; Field, M. J. *J. Phys. Chem. A* **2000**, 104, 4095.
- (14) Derepas, A.-L.; Soudan, J.-M.; Brenner, V.; Dognon, J.-P.; Millié, Ph. *J. Comput. Chem.* **2002**, 23, 1013.
- (15) Lefevre, R. J. W. *Advances in Physical Organic Chemistry*; Gold, V., Ed.; Academic Press: New York, 1965; Vol. 3, p 1.
- (16) Vigné-Maeder, F.; Clavier, P. *J. Chem. Phys.* **1988**, 88, 4934.
- (17) Stone, A. J.; Alderton, M. *Mol. Phys.* **1985**, 56, 1047.
- (18) Besler, B. H.; Merz, K. M., Jr.; Kollman, P. A. *J. Comput. Chem.* **1990**, 11, 431; (b) Singh, U. C.; Kollman, P. A. *J. Comput. Chem.* **1984**, 5, 129.
- (19) Kitaigorodskii, A. I. *Tetrahedron* **1961**, 14, 975.
- (20) Gresh, N. J. *Comput. Chem.* **1995**, 16, 856.
- (21) Bouvier, B.; Brenner, V.; Millié, Ph.; Soudan, J.-M. *J. Phys. Chem. A* **2002**, 106, 10326.
- (22) Stone, A. J. *Chem. Phys. Lett.* **1993**, 211, 101.
- (23) Fink, W. H. *J. Chem. Phys.* **1972**, 57, 1822. (b) Stevens, W.; Fink, W. H. *Chem. Phys. Lett.* **1987**, 139, 15.
- (24) Clavaguéra, C.; Hoyau, S.; Ismail, N.; Marsden, C. Submitted.
- (25) Andersson, K.; Barysz, M.; Bernhardsson, A.; Blomberg, M. R. A.; Carissan, Y.; Cooper, D. L.; Fleig, T.; Fülischer, M. P.; Gagliardi, L.; de Graaf, C.; Hess, B. A.; Karlström, G.; Lindh, R.; Malmqvist, P.-Å.; Neogrády, P.; Olsen, J.; Roos, B. O.; Schimmelpfennig, B.; Schütz, M.; Seijo, L.; Serrano-Andrés, L.; Siegbahn, P. E. M.; Ståhring, P. E. M.; Thorsteinsson, T.; Veryazov, V.; Wierzbowski, M.; Widmark, P.-O. *MOLCAS*, Version 5; University of Lund, Sweden, 2001.
- (26) Frisch, M. J.; Trucks, G. W.; Schlegel, H. B.; Scuseria, G. E.; Robb, M. A.; Cheeseman, J. R.; Zakrzewski, V. G.; Montgomery, J. A., Jr.; Stratmann, R. E.; Burant, J. C.; Dapprich, S.; Millam, J. M.; Daniels, A. D.; Kudin, K. N.; Strain, M. C.; Farkas, O.; Tomasi, J.; Barone, V.; Cossi, M.; Cammi, R.; Mennucci, B.; Pomelli, C.; Adamo, C.; Clifford, S.; Ochterski, J.; Petersson, G. A.; Ayala, P. Y.; Cui, Q.; Morokuma, K.; Malick, D. K.; Rabuck, A. D.; Raghavachari, K.; Foresman, J. B.; Cioslowski, J.; Ortiz, J. V.; Baboul, A. G.; Stefanov, B. B.; Liu, G.; Liashenko, A.; Piskorz, P.; Komaromi, I.; Gomperts, R.; Martin, R. L.; Fox, D. J.; Keith, T.; Al-Laham, M. A.; Peng, C. Y.; Nanayakkara, A.; Gonzalez, C.; Challacombe, M.; Gill, P. M. W.; Johnson, B. G.; Chen, W.; Wong, M. W.; Andres, J. L.; Head-Gordon, M.; Replogle, E. S.; Pople, J. A. *Gaussian 98*, Revision A.9; Gaussian, Inc.: Pittsburgh, PA, 1998.
- (27) Boys, S. F.; Bernardi, F. *Mol. Phys.* **1970**, 19, 553.

- (28) van Duijneveld, F. B. *IBM Res. Rep.* **1971**, RJ945.
- (29) Ismail, N.; Heully, J.-H.; Saue, T.; Daudey, J.-P.; Marsden, C. J. *Chem. Phys. Lett.* **1999**, *300*, 296.
- (30) Küchle, W.; Dolg, M.; Stoll, H. *J. Chem. Phys.* **1994**, *100*, 7535.
- (31) De Jong, W. A.; Vissher, L.; Nieuwport, W. C. *J. Mol. Struct. (THEOCHEM)* **1998**, *458*, 41. (b) De Jong, W. A.; Vissher, L.; Nieuwport, W. C. *J. Mol. Struct. (THEOCHEM)* **2002**, *581*, 259 (corrigendum).
- (32) Cornehl, H. H.; Heinemann, C.; Marçalo, J.; Pries de Matos, A.; Schwarz, H. *Angew. Chem., Int. Ed. Engl.* **1996**, *35*, 891.
- (33) (a) Poteau, R.; Spiegelman, F. *J. Chem. Phys.* **1993**, *98*, 6540. (b) Poteau, R.; Spiegelman, F. *J. Chem. Phys.* **1993**, *88*, 10089E.
- (34) Bertolus, M.; Brenner, V.; Millié, Ph.; Maillet, J.-B. *Z. Phys. D* **1997**, *39*, 239.
- (35) Fletcher, R. *Comput. J.* **1970**, *13*, 317. (b) Goldfarb, D. *Math. Comput.* **1970**, *24*, 23. (c) Shanno, D. F. *Math Comput.* **1970**, *24*, 647.
- (36) Ismail, N. Private communication.
- (37) Hoyau, S.; Ohanessian, G. *Chem. Eur. J.* **1998**, *4*, 1561. (b) Del Bene, J. E. *J. Phys. Chem.* **1996**, *100*, 6284.